

Rearward Forcing of an Unsteady Compressible Cascade

M. K. Fabian* and E. J. Jumper†
University of Notre Dame, Notre Dame, Indiana 46556

Phase-locked, steady and unsteady, surface pressure measurements were made on the vanes of a compressible cascade, for inlet Mach numbers up to ~ 0.7 . The cascade vanes were production hardware stator vanes from an AlliedSignal F109 turbofan engine. Data are presented from which it may be concluded that the cascade produces reasonably good two-dimensional flow through the vane row. Unsteady forcing within the cascade can be produced either upstream or downstream of the vane row. In the present paper, flow unsteadiness in the cascade was produced using shedding from circular cylinders positioned at a distance equal to 80% vane chords downstream of the vane row. This rearward forcing of the vane row resulted in unsteady surface pressures of the same order as those produced in similar experiments with forward forcing. Decomposition of the ensembled, phase-locked, pressure-response signals for rearward forcing provided insight into both the nature of the unsteady disturbance and the physics of its propagation within the vane row.

Nomenclature

A	= signal amplitude
a	= speed of sound
C_p	= compressible coefficient of pressure
C_{p0}	= incompressible coefficient of pressure
c	= cascade-turning vane chord
f	= signal frequency
M	= Mach number
P	= static pressure
\bar{P}	= unsteady pressure
P_0	= total pressure
t	= time
U	= axial velocity
x	= distance from vane leading edge
γ	= specific heat ratio
Φ	= signal phase
Φ_t	= vane trailing-edge phase delay
ω	= angular frequency

Subscripts

h	= harmonic frequency quantity
L	= local quantity
p	= primary frequency quantity
∞	= freestream quantity

Superscript

$^\circ$	= degrees
----------	-----------

Introduction

A RECENT U.S. Air Force initiative in high cycle fatigue (HCF) has a stated goal of eliminating HCF as a major cause of engine failures. The perplexing nature of HCF failures is that they are unanticipated. A portion of these failures may ultimately be traced to foreign object damage (FOD), or other specific causes; however, more often they are a result of un-

expected component failure and, as such, remain unexplained. One component of the science and technology portion of the HCF program is directed toward improved forced-response prediction in the hope that better predictive capabilities might be able to explain and prevent unanticipated component failure. Such predictions will mainly depend on numerical simulations of the unsteady flow and unsteady pressure response of the various aerodynamic components integral to turbomachines. Numerical simulations require experimental data for the purposes of code validation. These data must include both detailed, time-resolved, unsteady, pressure response at engine operating conditions, as well as concomitant boundary conditions. As will be discussed briefly below, although low-speed, essentially incompressible response data are plentiful, there is a paucity of detailed compressible data caused by upstream forcing (caused, for example, by vortical disturbances); compressible data caused by downstream forcing, i.e., rearward forcing, is almost nonexistent. This latter forcing method in compressible flows is, by its nature, potential. In fact, many of the existing response codes treat only convectively transported vortical disturbances. It is, therefore, of interest to document the extent and character of unsteady pressure response on a vane row caused by potential disturbances generated downstream of the row.

This paper focuses on the results obtained from time-resolved, unsteady, surface pressure measurements made on the turning vanes of a transonic cascade. The results represent the first phase of a multiphase investigation of the stator vanes, with subsequent phases investigating their response installed in an AlliedSignal F109 turbofan engine. In anticipation of the engine tests, instrumented F109 stator vanes were fitted as turning vanes in a transonic cascade facility. The cascade testing had several objectives that included testing the structural integrity of the instrumented vanes, and verifying instrument operation at actual engine forcing frequencies, mass-flow rates, and Mach numbers. Additionally, cascade tests provided an opportunity to characterize the unsteady pressure response of the vanes in a cascade that simulated actual engine operating conditions; a portion of the results of the cascade experiments are reported on here.

The cascade facility is unique in two ways: first, the cascade operates in the compressible flow regime up to transonic; second, the unsteady forcing can be accomplished from either upstream or downstream of the stator vane row. Many previous unsteady cascade and compressor-rig experiments have involved only incompressible flows,^{1–6} with only limited public-domain data being available for unsteady, compressible cas-

Received Aug. 4, 1997; revision received June 15, 1998; accepted for publication June 23, 1998. Copyright © 1998 by M. K. Fabian and E. J. Jumper. Published by the American Institute of Aeronautics and Astronautics, Inc., with permission.

*Graduate Research Assistant, Hessert Center for Aerospace Research, Department of Aerospace and Mechanical Engineering; currently Assistant Professor, Department of Aeronautics, U.S. Air Force Academy, CO 80840. Member AIAA.

†Professor, Hessert Center for Aerospace Research, Department of Aerospace and Mechanical Engineering. Associate Fellow AIAA.

cares.^{7,8} Furthermore, an extensive open-literature search found only two experimental studies that considered forcing from downstream.^{9,10} The first of these studies reported on simultaneous upstream and downstream forcing at very low Mach numbers, and drew essentially no conclusions regarding the importance of downstream forcing.⁹ The second study considered downstream forcing exclusively; however, only low-speed, incompressible results were examined.¹⁰ In the present paper, we provide new, compressible-cascade, pressure-response data for unsteady forcing exclusively from downstream sources. Further, analysis of these data will attach special significance to the relative phase information that provides insight into the propagation nature and importance of the disturbances.

Facilities and Equipment

The cascade used for this research effort, as shown in Fig. 1, formed the test section of one of three transonic, in-draft, wind tunnels located in the Hessert Center for Aerospace Research at the University of Notre Dame. The cross-sectional dimensions of the cascade are $0.1003 \text{ m} \times 0.1003 \text{ m}$, allowing for five flow passages formed from six vanes, two of which blended with the end walls of the cascade. The resultant five flow passages meet the periodicity conditions through the central passage for a subsonic cascade, as described by Oates.¹¹

Cascade Turning Vanes

As stated previously, the cascade turning vanes are production hardware stator vanes from the F109 engine. The vanes have a double circular arc airfoil section with a maximum camber and thickness of 12 and 8% chord, respectively. The vanes have a slightly varying chord from tip to hub, but they have no twist. The nominal vane chord length is 3.25 cm and the vane spacing is 2.13 cm. The 42.5-deg cascade turning angle represents an average value of the design 39.8- and 45.2-deg stator tip and hub turning angles for the F109. In the F109, the stators are swept aft from hub to tip; however, in the cascade their leading edges are positioned normal to the flow direction, forming a nominal two-dimensional cascade.

A total of 16 stator vanes were instrumented along chord lines at two engine axis positions, as shown in Fig. 2. Because of the small leading-edge radius and cusped trailing edge of the vanes, surface pressure measurements were limited to vane pressure surface and suction surface locations at 7, 12, 20, 30, 40, 50, 65, and 80% chord. Space limitations allowed for (at most) two pressure taps per vane; therefore, each vane was instrumented with one pressure surface and one suction surface pressure tap.

Kulite XCS-062 pressure transducers were imbedded within the vanes so that the transducer head formed one surface of a small cavity directly below the surface pressure tap. As such,

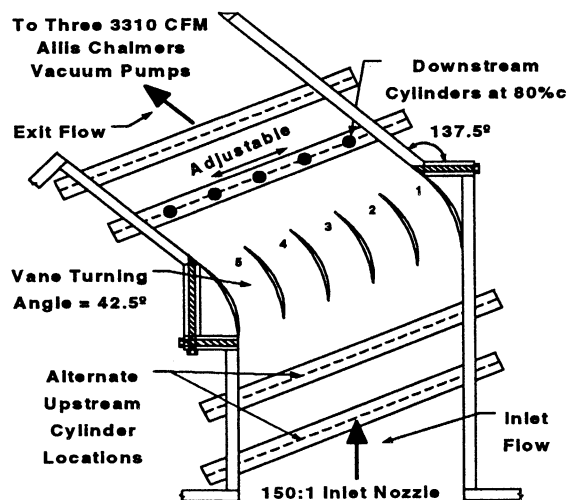


Fig. 1 Top view of cascade test section.

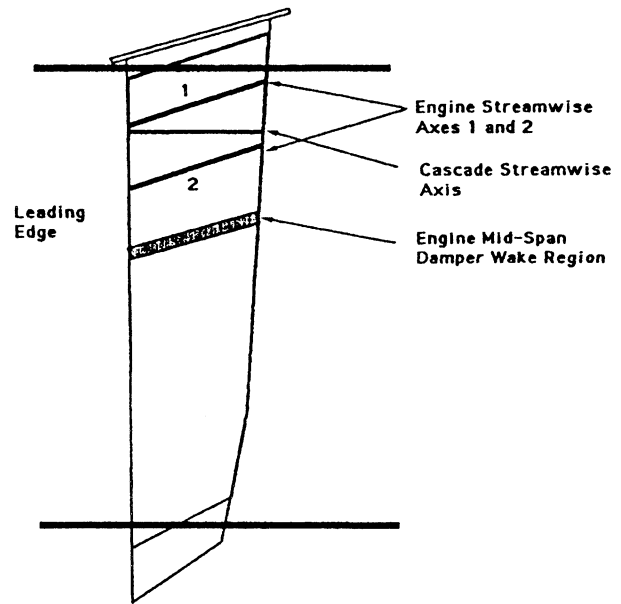


Fig. 2 Side view of stator.

the transducers were essentially surface mounted. The transducers had 35-kPa differential flat dynamic responses in excess of 20 kHz; the internal cavity dimensions were analyzed and found to have natural frequencies of approximately 50 kHz. In addition, the characteristic frequencies associated with the cascade were analyzed for the transducers, using the standard practice set forth by Figliola and Beasley,¹² and were found to yield essentially a unity transfer function through 20 kHz.

Additionally, four specially designed vanes were each instrumented with 15 chordwise pressure taps via a remotely mounted scanivalve to acquire steady flow and time-averaged pressure data. These scanivalve-instrumented vanes were constructed of epoxy-resin cast with internal stainless-steel tubing in molds made from the F109 stator vanes. Because of the limited thickness of the vanes, and consideration of the location of the wake region from the F109 fan midspan dampers, instrumentation locations were restricted, with two vanes instrumented along engine axis 1, one vane instrumented along engine axis 2, and the last vane instrumented along a cascade axis, as shown in Fig. 2.

Unsteady Forcing

Unsteady forcing of the turning vanes was established through vortex shedding from a row of five circular cylinders. The cylinders could be placed either upstream or downstream of the vane row, at a distance of 0.8 or 1.6 vane chords from the leading or trailing edge of the vanes (Fig. 1). The cylinders were aligned normal to the oncoming flow (parallel to the vane spans), with the same spacing as the vane row, and could be adjusted in the direction normal to the vane spans. Note that all unsteady data presented here are for rearward forcing, with the cylinders located at 0.8 vane chords downstream of the vane trailing edges, and aligned with the midpassages of the vane row (Fig. 1).

The diameter of the cylinders could be varied to adjust the cylinder shedding frequency. Over the range of Reynolds numbers in the experiment (from 2×10^4 to 6×10^4 , based on cylinder diameter), the Strouhal number was constant at approximately 0.2. Thus, the reduced frequencies (based on vane half-chord) were fixed once a cylinder diameter was selected. The results reported here are from 4.7-mm-diam forcing cylinders, corresponding to a reduced frequency of approximately 4.5 over the entire range of Mach numbers tested. Reduced frequency is given by

$$\tilde{f} = fc/2U_\infty \quad (1)$$

where \tilde{f} is the reduced frequency, f is the frequency, c is the vane chord, and U_∞ is the freestream velocity.

Phase-Locked Data Acquisition

All unsteady pressure measurements presented here were acquired through conditional sampling techniques based on the initiation of a trigger signal. Initiation of the trigger signal occurred when a transducer embedded in one of the circular cylinders measured a specified minimum pressure amplitude on the surface of the cylinder, as a result of vortex shedding, after a positive crossing of the zero voltage range.¹ It should be noted, as with Commerford and Carta,¹ that sufficient periodicity was present in the shedding to provide ensemble results and determine the flow, unsteady, aerodynamic characteristics for each cascade frequency and Mach number combination.

Data were collected using an RC-Electronics IS-16E, high-speed, data acquisition and A/D card with a Nyquist frequency of 125 kHz, as configured. A Measurements Group Model 2300 signal conditioner provided the 15-V transducer excitation and amplified the transducer output. In addition, a manometer bank was used to measure static and total pressure upstream of the cascade test section to determine the cascade inlet Mach number.

Steady Flow Results

In this section, C_p data are presented for the cascade in an unforced state, i.e., with no unsteady flow generators installed in the cascade. These data demonstrate the cascade flow quality.

Engine Axis 1, Steady, C_p Data

Using a remotely mounted scanivalve, as detailed earlier, steady vane pressure data were acquired at 15 vane, chordwise, pressure-tap locations along engine axis 1, as shown in Fig. 2, for a range of inlet Mach numbers. Figure 3 gives an overlay of steady-flow data, reduced to C_p using the cascade inlet M_∞ and P_∞ , for 12 inlet Mach numbers ranging from 0.202 to 0.694. Note that the data in Fig. 3 have been reduced to an equivalent, Mach zero, incompressible C_{p0} using the Prandtl-Glauert transformation. Except for the Mach 0.694 data, Fig. 3 shows that the C_{p0} data are nicely behaved. Additionally, data for any Mach number up to 0.6 may be obtained via an average

C_{p0} distribution made up of all the equivalent Mach zero data. Note the 95% confidence interval bar; error analysis details may be found in Ref. 13. As such, it may be inferred that Reynolds number effects, while present, do not affect the data.

The well-behaved character of these data suggest that the cascade has a fully attached flow at least up to Mach 0.6. Attached flow was also inferred from surface-oil flow visualization studies.¹³ It should be noted that these flow visualization studies showed that even at the engine axis 1 location, the end wall had essentially no effect on the cascade axis, two-dimensional nature of the flow. The pressure data of Fig. 3 may also indicate a shock-induced separation region over the suction side of the vanes for the Mach 0.694 data. These Mach 0.694 data, along with other measurements and cascade analysis not reported on here, indicate that the cascade becomes transonic and can experience shocks for inlet Mach numbers greater than 0.6.

Two-Dimensional Flow Quality and Airfoil Geometry Sensitivity

Figure 4 gives an overlay of C_p data at Mach 0.4 for the four, 15-tap, scanivalve-instrumented vanes. It may be inferred from Fig. 4 that the flow in the cascade is essentially two dimensional because of the relative agreement between the data taken at the separate spanwise locations. It is important, however, to address the data scatter shown in Fig. 4. Setting aside bias error, the uncertainty in any single data point is small. The 512 samples for each data point have a standard deviation of approximately $0.002C_p$, which is smaller than the data symbols shown in Fig. 4. If any bias error is present for a given vane, because a scanivalve was used, that bias is common to all 15 vane taps. To minimize bias error between vanes, calibrations were performed on the scanivalve pressure transducer prior to each run. Over all data sets, including those not reported here, the calibration coefficients varied by less than 1%.

Also of note, each chordwise, alternating, engine axis 1, data point shown in Fig. 4 was acquired by one or the other of the two, 15-tap, engine axis 1 vanes. The fact that the data differs by as much as 20% between vanes, and appears to be a consistent variation, cannot be attributed to a lack of flow two dimensionality in the cascade, for two reasons. Firstly, the vane, spanwise, 15-tap locations for each vane lie along identical engine axis rays, i.e., location 1 in Fig. 2. Secondly, data

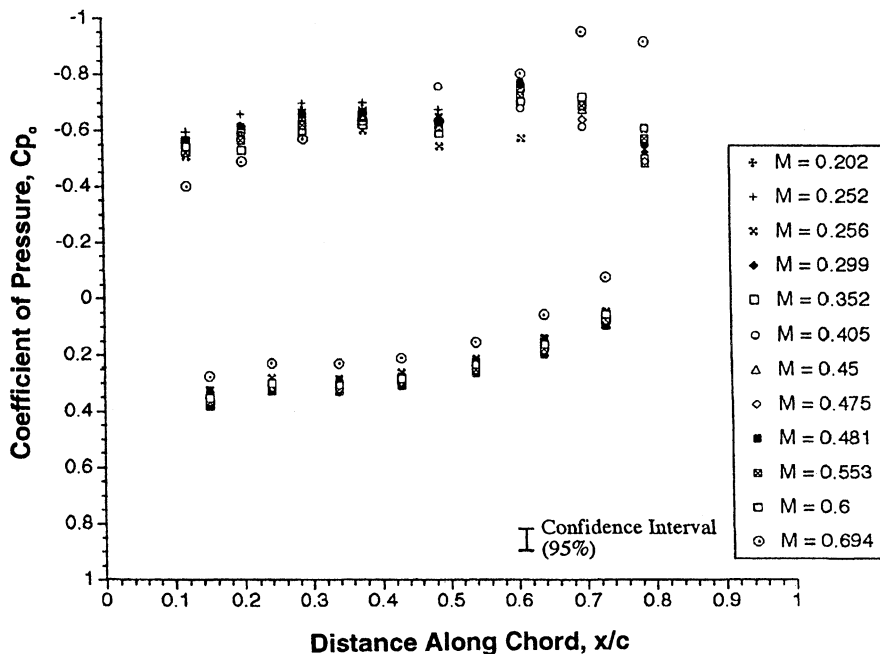


Fig. 3 Mach number sweep of clean tunnel configuration.

runs were made for each of the four 15-tap vanes, and the eight composite vanes, at cascade vane locations 3 and 4 (Fig. 1). The data from these runs, for the same vane (both steady and time averaged), showed virtually no variation between locations.

Because non-two-dimensional effects can be discounted, it is clear that some other factor, or factors, must be responsible for the data scatter. It has long been known that airfoil geometry variations have a large effect on a given flowfield. Hawthorne¹⁴ specifically warns that such geometry-induced variations will be present in cascade data when the turning vane chords are as small as those used in this study. Inspection of the four 15-tap vanes and the 16 instrumented vanes showed both camber and thickness variations between vanes. Most of these variations were small; however, relatively large variations were noted on the eight Kulite-instrumented vanes for engine axis 1. Fixing the trailing edges of the two most dissimilar vanes produced a leading-edge discrepancy between

vanes of 0.5% chord. Inspection of the two engine axis 1 scanivalve instrumented vanes showed only minute, almost imperceptible variations; however, Fig. 4 underscores the sensitivity of the pressure data to these geometry variations. Angle-of-attack variations may also be present from one vane to the next; however, these were minimized by the way in which the vanes were held in the cascade. Additionally, virtually no difference in C_p data, for a given vane, was noted by placing it at either cascade vane locations 3 or 4 (Fig. 1).

Thus, it is our opinion that the variation between the two, 15-tap, engine axis 1 vanes is a result of slight variations in their geometry. Further, because the scatter between data from the 15-tap engine axis 2 vane, the cascade axis vane, and one of the engine axis 1 vanes is not greater than the scatter between the two engine axis 1 vanes, we also attribute the scatter between all of the data in Fig. 4 to primarily be a result of geometry variations between vanes.

Unsteady Flow Results

Forcing Gust

As described earlier, unsteady gusts were produced from shedding off five circular cylinders. The spanwise cylinder locations were varied and the resulting vane unsteady pressure response was examined. In general, the response was independent of cylinder alignment location; however, placement of the forcing rods at the midpassage location between vanes yielded the cleanest response signals. Thus, all data presented here were taken for midpassage alignment of the forcing rods.

As discussed in a separate paper, the gust produced by the cylinder vortex shedding is made up of two parts: a potential portion because of bound circulation, and a convected portion because of free vorticity shed downstream into the convecting wake.¹⁵ From the data collected, it appears that, at least where the vanes are instrumented, the potential and convective disturbances are two dimensional with regard to span direction and are synchronized (phase-locked) from one cylinder to another. This was demonstrated by three specific examinations. Firstly, the phase information obtained from unsteady pressure signals was nearly identical, when measured at a given chord location, along either engine axes 1 or 2. Secondly, signals measured at the same chord locations, but with the trigger cylinder located at different locations in the forcing row, were virtually identical. Thirdly, vane row locations yielded passage-to-passage periodicity by holding the trigger location

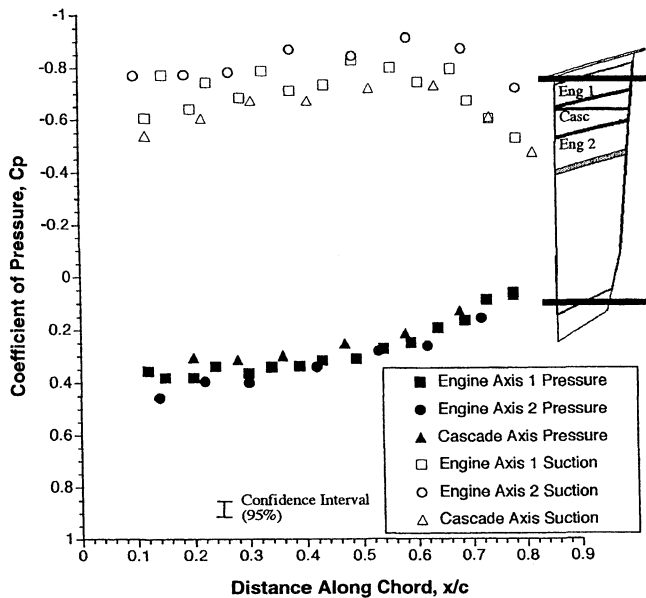


Fig. 4 Comparisons of engine-based instrumentation axes with cascade axis, all data based on scanivalve profiles of cast resin blades, $M_{inf} = 0.4$.

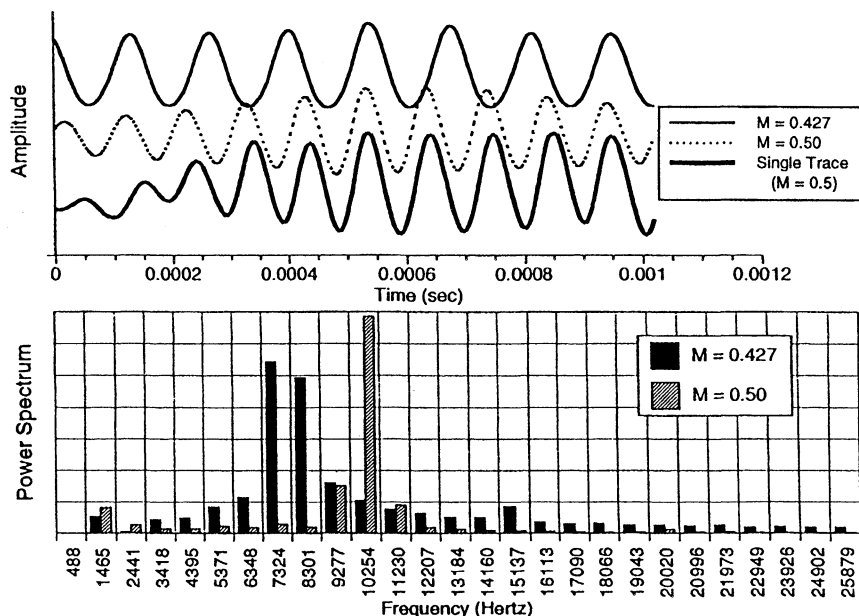


Fig. 5 Trigger time history and power spectrum with rods rearward for $M = 0.427$ and $M = 0.50$, and sample trigger trace at $M = 0.50$.

fixed and shifting the instrumented vanes within the cascade row.

The gust periodicity in time was examined by studying the trigger signal used to phase-lock the vane response. Figure 5 gives trigger signals and their power spectral densities (PSDs) for two Mach number cases. The PSD plots show that the primary forcing, or fundamental, signal is a fairly narrow band. The tailing off of the 400 ensemble-averaged signal from the center locking point, which is most noticeable for the $M_\infty = 0.50$ signal trace in Fig. 5, is a result of a modulation of the signal amplitude at all Mach numbers and is, in fact, present on all of the signals. This modulation does not appear to be an artifact of the ensemble averaging because individual, non-averaged, traces show the same modulation, as can be seen in Fig. 5 for the single-trace signal, also for $M_\infty = 0.50$. The low-frequency modulation is at nearly the same frequency for all Mach numbers, ~ 1700 Hz, which may indicate some mechanical vibration mode or vacuum-pump mode, characteristic of the transonic facility.

Unsteady Pressure Response

Figure 6 shows the normalized root-mean-square (rms) fluctuating pressure as a function of chordwise location, on both the vane suction and pressure sides, for rearward forcing at Mach numbers from 0.427 to 0.5, with a normalizing pressure of 6.89 kPa (or 1 psi). The fluctuating pressure represents phase-locked, 400-ensemble, unsteady, pressure signals from eight instrumented vanes with the mean, or dc, component removed. The data-point displacement from the airfoil surface in Fig. 6 is the normalized, rms, pressure amplitude for each chordwise location.

It should be noted for the unsteady pressure data presented here, i.e., Figs. 6 and 7, that under the assumption that the variation of any single time series from that of its corresponding ensemble series is random, then the 400-ensemble signals represent the true expected values. Also, the use of 400 ensembles gave less than 0.1% rms error relative to that from 1000 ensembles, whereas the rms unsteady pressures of all individual time series were consistently $\sim 30\%$ higher than the 400-ensemble, rms, unsteady pressure. This was primarily because of a slight phase shifting from one time series to the next. Thus, the reported rms unsteady pressures are conservative in the sense that they underreport the actual rms unsteady pressure by approximately 30%; the relative magnitudes of the rms unsteady pressures remain the same.

The data shown in Fig. 6 may be compared with similar data obtained for forward forcing, as presented by Fabian and

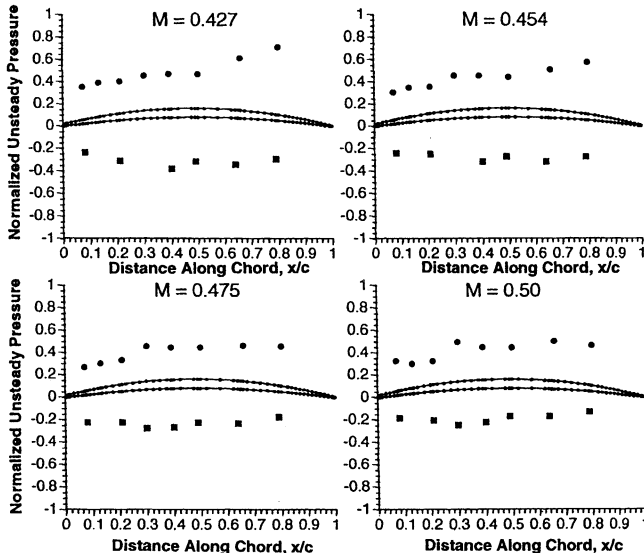


Fig. 6 Root-mean-square pressures for rods rearward (uncertainty referenced in text).

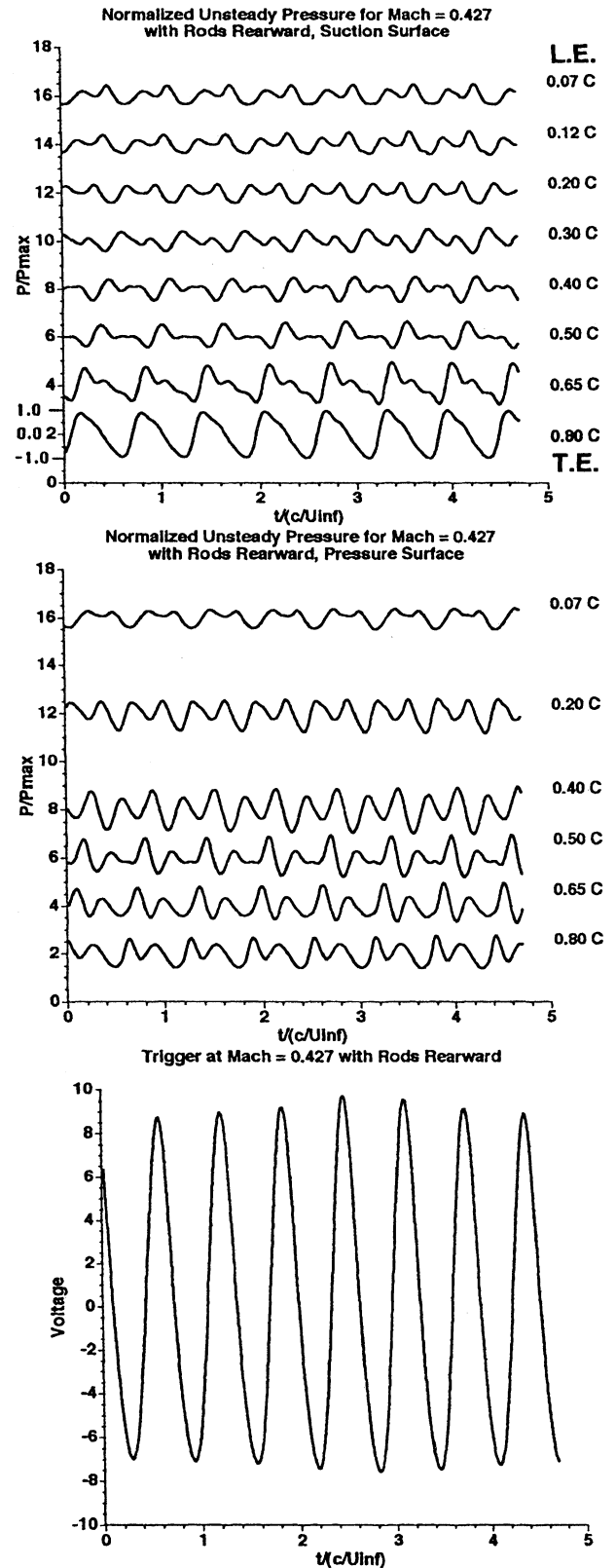


Fig. 7 Signal averages for $M = 0.427$ (uncertainty referenced in text).

Jumper.¹⁶ From this, one may note that the unsteady pressure disturbances measured on the vanes from rearward forcing are nearly equal in magnitude to those measured from forward forcing. This is surprising because, in the case of forward forcing, although the potential disturbances caused by fluctuating bound circulation on the forcing cylinders should be similar to

those for rearward forcing, the disturbances radiate downstream along with the cylinder's convecting wakes. In the case of rearward forcing, however, only the potential disturbances interact with the vane row, as they can radiate at acoustic speed upstream into the oncoming flow, as long as the flow is subsonic.

Figure 7 shows normalized, phase-locked, 400-ensemble, unsteady, pressure signals for the Mach 0.427 case. In addition to the ensembled trigger signal, the normalized unsteady pressure is plotted vs nondimensional time, i.e., tU_∞/c , for the vane suction surface and pressure surfaces. These data are representative of all Mach number cases. Table 1 gives the normalizing pressures for the pressure and suction surfaces shown in Fig. 7.

From Fig. 7, it is apparent that although the primary frequency of the response data is at the forcing frequency, the response curves have additional structure. A similar structure has been noted in stator response signals from incompressible rotating machines,⁵ in which it was noted that the structure could be decomposed into a primary frequency sinusoidal response plus a harmonic sinusoidal response. Thus, each of the 14 response curves in Fig. 7 (eight suction curves and six pressure curves) was decomposed into its primary and harmonic sinusoidal response using an optimization routine.¹³

Table 2 gives the relevant parameters of the 14 decompositions, one for each vane chord location. Any particular vane chord location signal may be reproduced from these parameters from

$$\tilde{P} = A_p \sin(2\pi f_p t + \Phi_p) + A_h \sin(2\pi f_h t + \Phi_h) \quad (2)$$

Figure 8 illustrates how well Eq. (2) reproduces the structure of a given signal using the decomposition parameters of Table 2.

With the decomposition information, it was possible to construct Figs. 9a and 9b. These figures show the decomposed, primary and harmonic, normalized response, as a function of time, and displaced along the vertical scale to reflect relative chord position. From Figs. 9a and 9b, it is clear that an unambiguous, nearly straight-line, phase relationship exists between the primary and harmonic response signals, respectively. In addition, the phase relationships for the primary and har-

monic signals clearly indicate wave propagation from the trailing edge to the leading edge of the vanes.

Using a linearized theory, it is possible to predict the upstream phase lag of an acoustically propagating, potential disturbance emanating from a downstream forcing source.^{13,15} It is known that the effects of a change in the downstream aerodynamic forcing field, resulting from a change in the bound circulation on the forcing rods, are time delayed in the upstream aerodynamic field because of propagation at the local speed of sound. Thus, it can be shown that the field response at some distance directly upstream from a sinusoidal circulation source (at a location, x , from the leading edge of a vane with chord, c) in a flow of Mach number, M_∞ , should be felt in the field as

$$\sin \left[\omega t + \Phi_i - \frac{(c-x)\omega}{a_\infty(1-M_\infty)} \right] \quad (3)$$

Note that the phase shift is both Mach number and frequency dependent.

Two theoretical curves are shown in Fig. 10 for the primary and harmonic phase shift predicted from the simple linearized theory of Eq. (3), as a function of relative vane chord and assuming a Mach number of 0.59. Also overlaid in Fig. 10 are experimentally measured primary and harmonic phase data, for the suction side of a nominal vane, taken at a cascade inlet Mach number of 0.427. The agreement between the theoretical and experimental phase data of Fig. 10 show that the primary and harmonic phase shifts may be inferred to be a result of a signal emanating from the same source and propagating upstream through the same average Mach 0.59 flow.

Similarly, the predicted and experimental phase shifts for the pressure side of the vane are shown in Fig. 11. This figure

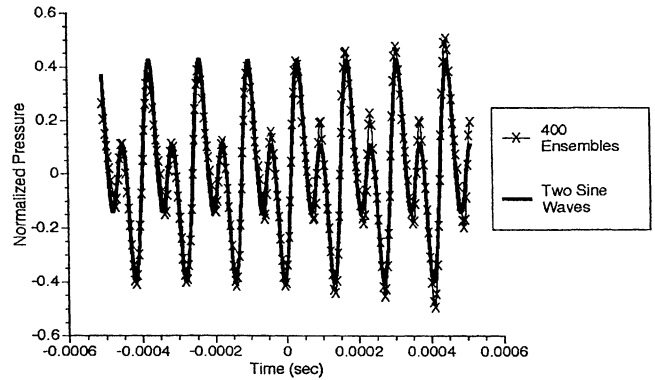


Fig. 8 Four-hundred ensembles at 30% C , suction surface at $M = 0.427$ with rods rearward vs two sine waves, $0.206 \sin(2\pi 7262t - 0.636) + 0.260 \sin(2\pi 14524t - 1.464)$.

Table 1 Normalizing amplitude for signal traces

Cascade inlet Mach number	Suction surface, Pa	Pressure surface, Pa
0.427	5812.3	4564.3
0.454	2420.1	1723.7
0.475	1496.2	1461.7
0.500	2268.4	1454.8

Table 2 Amplitude and phase for Mach 0.427, primary frequency = 7280 Hz

x/c position	Primary amplitude, Pa	Primary phase, rad	First harmonic amplitude, Pa	First harmonic phase, rad	rms error of fit, Pa
0.07 suction	1261.7	2.415	1303.1	0.659	372.3
0.12 suction	1234.2	2.874	1496.2	1.699	386.1
0.20 suction	1089.4	-2.027	1613.4	-2.603	268.9
0.30 suction	1261.7	-0.636	1585.8	-1.464	296.5
0.40 suction	1241.1	0.413	1675.4	1.372	441.3
0.50 suction	1379.0	1.638	1634.1	2.964	517.1
0.65 suction	2840.6	3.158	1772.0	0.067	96.5
0.80 suction	5178.0	-2.454	1365.2	1.476	510.2
0.07 pressure	1268.6	2.625	951.5	0.168	158.6
0.20 pressure	979.1	-2.257	2282.2	3.038	344.7
0.40 pressure	1096.3	-1.580	3137.1	-0.667	310.3
0.50 pressure	792.9	-1.302	2185.6	1.182	848.1
0.65 pressure	772.2	-1.591	2323.5	2.889	786.0
0.80 pressure	1268.6	-1.694	1840.9	-1.714	627.4

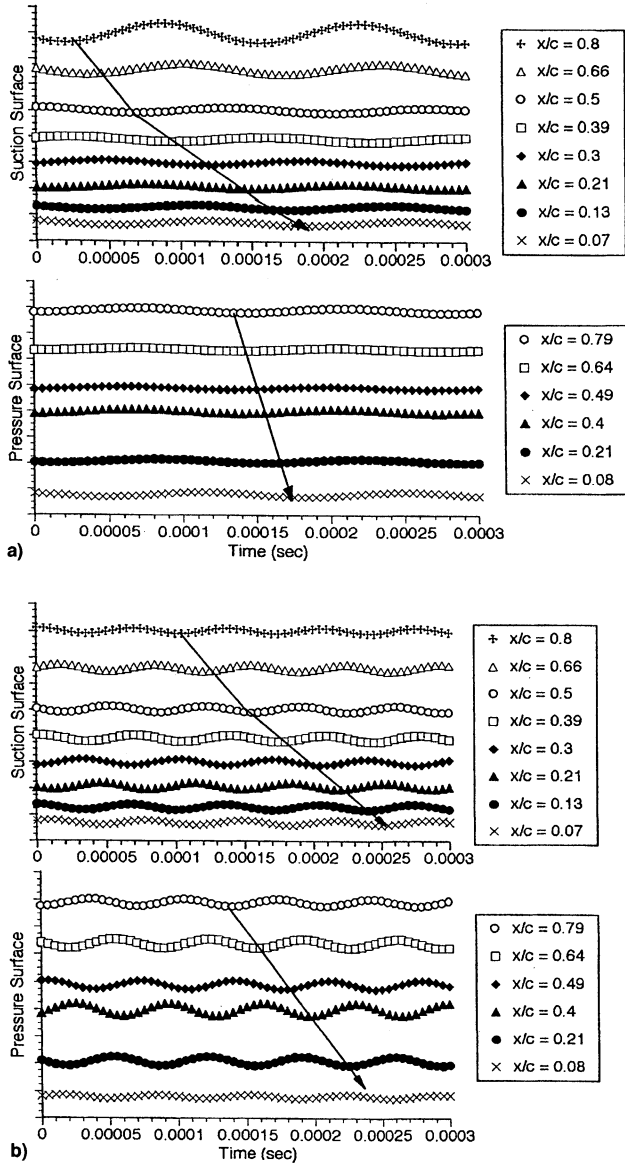


Fig. 9 a) Primary mode and b) first harmonic on suction and pressure surfaces for rods rearward, $M = 0.427$, normalized to largest value and shifted by relative x/c .

indicates that the propagation direction is also unambiguously inferred to be from the same downstream origin, propagating upstream into an oncoming flow, but now at an average Mach number of 0.35. These inferred average Mach numbers of 0.59 over the suction surface, and 0.39 over the pressure surface, are in excellent agreement with the Mach numbers derived from the vane, time-averaged, pressure data using

$$M_L = \sqrt{\frac{2}{\gamma - 1} [(P_0/P_L)^{(\gamma - 1)/\gamma} - 1]} \quad (4)$$

A plot of the local Mach numbers, M_L , derived from the vane, time-averaged, pressure data is given in Fig. 12. Such excellent agreement between the phase and Mach number data was found, at both engine axes, for all of the rearward-forced cases.

It should be noted that the experimental uncertainty in the phase data of Figs. 10 and 11 directly corresponds to the error associated with the decomposed representation of the ensemble data, as shown in Fig. 8. As such, the rms error reported in Table 2 provides an approximate measure of the uncertainty in any given decomposed data.

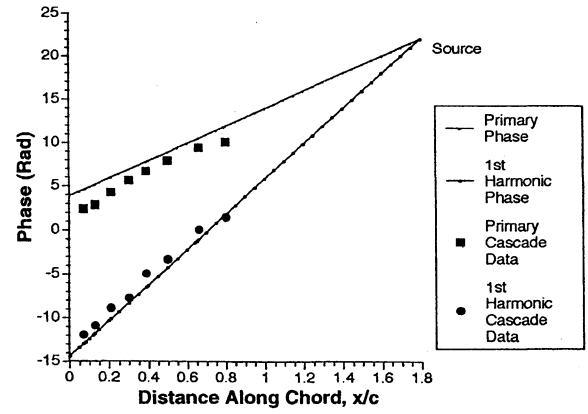


Fig. 10 Suction surface upstream traveling wave for primary forcing frequency of 7280 Hz and first harmonic with Mach 0.59 compared with data from rods downstream case with $M_{inlet} = 0.427$.

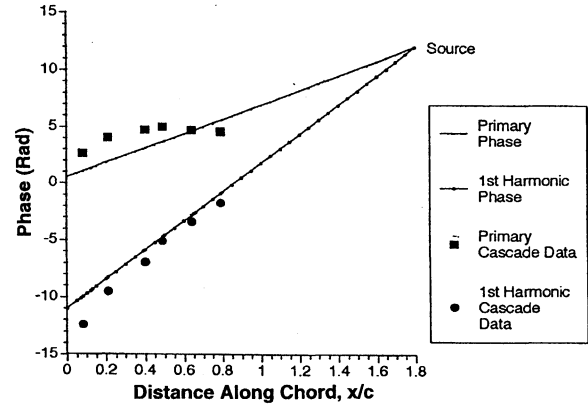


Fig. 11 Pressure surface upstream traveling wave for primary forcing frequency of 7280 Hz and first harmonic with Mach 0.35 compared with data from rods downstream case with $M_{inlet} = 0.427$.

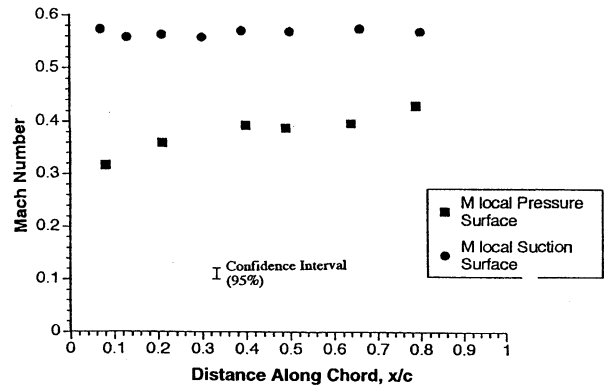


Fig. 12 Local Mach number vs chord position for $M_{inlet} = 0.427$ with rods rearward.

Discussion

The inference drawn from the phase data of the rearward-forced, unsteady, pressure responses is unambiguous; the unsteady pressure response over the vanes is a result of a disturbance propagating at acoustic speed into the oncoming flow. The well-behaved nature of the phase data further suggests that the quality of the cascade is reasonably good. The fact that the data exhibits such well-behaved phase information may not in itself seem surprising; however, almost without exception, phase information found in the literature is not well behaved.¹⁷

Also of note, the unambiguous propagation direction inferred from the phase data may be drawn from either the primary or harmonic frequency results; however, the arguments leading to Eq. (3) were based on the existence of alternating bound circulation on the forcing cylinders. The trigger signal shown in Fig. 7 is a direct measure of the periodicity of this circulation and appears to contain only primary (forcing) frequency information. At a distance of many cylinder diameters upstream from the forcing cylinders, i.e., at the vane row, this alternating bound circulation will give rise to a fluctuating component of velocity approximately normal to the mean flowfield.¹⁵ Thus, it is reasonable to assume that the unsteady pressure response of the vane row, at the primary frequency, is a result of velocity fluctuations that are approximately normal to the surface of the vanes.

Consequently, because the phase data indicate that the harmonic disturbances also emanate from the forcing cylinder, and yet there appears to be no sign of a harmonic in the trigger signal, it seems reasonable to question the origin of the harmonic disturbance. The simplest explanation for its origin is the production and shedding of two, alternating-sense, free vortices into the cylinder wake for every single oscillation of bound circulation around the cylinder. These alternating-sense vortices each produce one cycle in drag fluctuation, thereby producing a drag fluctuation frequency at twice the primary frequency. If this is true, the harmonic disturbance is a result of a fluctuation in the velocity in a direction parallel to the mean flow, caused by the unsteady drag on the forcing cylinders.

Assuming these hypotheses about the nature of the primary and harmonic disturbances are correct, the unsteady pressure response of the vanes, at the primary and harmonic frequencies, are because of fundamentally different types of disturbances. It is interesting to note that, while not presented here, the response amplitude of the vanes exhibit very different characters at the primary and harmonic frequencies. A more detailed analysis of the character of the response amplitudes is addressed in a separate article.¹⁶

Conclusions

In this paper, an unsteady transonic cascade has been described that incorporates production hardware stator vanes from an AlliedSignal F109 turbofan engine as turning vanes. Steady data were presented that show the cascade to be essentially two dimensional and the quality of the data derived from the cascade is good. The unsteady data, caused by forcing of the vane row from downstream, were also presented and shown to be of good quality. These rearward-forced data demonstrated two points. First, the unsteady response of the vanes, caused by rearward forcing of the vane row, is essentially of the same magnitude as that for forward forcing of the vane row. Second, the nature of the response phase data demonstrates, unambiguously, that the disturbances are potential and propagate acoustically; they are, therefore, acoustic disturbances.

It should be noted that the question of whether or not the acoustic disturbance is propagating or evanescent is irrelevant as far as its ramifications toward unsteady forced response. The disturbances are clearly capable of producing unsteady pressure responses on the vane with magnitudes on the order of

those produced by similar means from upstream in the cascade. As such, these data have specific relevance to the stage-to-stage interaction problem.

Acknowledgments

This research effort was jointly sponsored by the Turbine Engine Division of the Aero-Propulsion and Power Directorate at Wright-Patterson Air Force Base, the Aerospace and Mechanical Engineering Department at the University of Notre Dame, and the Department of Aeronautics at the U.S. Air Force Academy. The U.S. Government is authorized to reproduce and distribute reprints for Governmental purposes notwithstanding any copyright notation thereon.

References

- ¹Commerford, G. L., and Carta, F. O., "Unsteady Aerodynamic Response of a Two-Dimensional Airfoil and High Reduced Frequency," *AIAA Journal*, Vol. 12, No. 1, 1974, pp. 43-48.
- ²Dring, R. P., Joslyn, H. D., and Hardin, L. W., "An Investigation of Axial Compressor Rotor Aerodynamics," *Journal of Engineering for Power*, Vol. 104, Jan. 1982, pp. 84-96.
- ³Zierke, W. C., and Okiishi, T. H., "Measurement and Analysis of Total-Pressure Unsteadiness Data from an Axial-Flow Stage," *Journal of Engineering for Power*, Vol. 104, April 1982, pp. 479-488.
- ⁴Gallus, H. E., Lambert, J., and Wallmann, T., "Blade-Row Interaction in an Axial Flow Subsonic Compressor Stage," *Journal of Engineering for Power*, Vol. 102, Jan. 1980, pp. 169-177.
- ⁵Fleeter, S., Jay, R. L., and Bennett, W. A., "Rotor Wake Generated Unsteady Aerodynamic Response of a Compressor Stator," *Journal of Engineering for Power*, Vol. 100, Oct. 1978, pp. 664-675.
- ⁶Fleeter, S., Jay, R. L., and Bennett, W. A., "The Time-Variant Aerodynamic Response of a Stator Row Including the Effects of Airfoil Camber," *Journal of Engineering for Power*, Vol. 102, April 1980, pp. 334-343.
- ⁷Hathaway, M. D., Gertz, J. B., Epstein, A. H., and Strazisar, A. J., "Rotor Wake Characteristics of a Transonic Axial-Flow Fan," *AIAA Journal*, Vol. 24, No. 11, 1986, pp. 1802-1810.
- ⁸Epstein, A. H., Gertz, J. B., Owen, P. R., and Giles, M. B., "Vortex Shedding in High-Speed Compressor Blade Wakes," *Journal of Propulsion and Power*, Vol. 4, No. 3, 1987, pp. 236-244.
- ⁹Schmidt, D. P., and Okiishi, T. H., "Multistage Axial-Flow Turbomachine Wake Production, Transport, and Interaction," *AIAA Journal*, Vol. 15, No. 8, 1977, pp. 1138-1145.
- ¹⁰Ng, W. F., O'Brien, W. F., and Olsen, T. L., "Experimental Investigation of Unsteady Fan Flow Interaction with Downstream Struts," *Journal of Propulsion and Power*, Vol. 3, No. 2, 1987, pp. 157-163.
- ¹¹Oates, G. C., *Aerothermodynamics of Gas Turbine and Rocket Propulsion: Revised and Enlarged*, AIAA Educational Series, AIAA, Washington, DC, 1988.
- ¹²Figliola, R. S., and Beasley, D. E., *Theory and Design for Mechanical Measurements*, Wiley, New York, 1991.
- ¹³Fabian, M. K., "Unsteady Pressure Distributions Around Compressor Vanes in an Unsteady, Transonic Cascade," Ph.D. Dissertation, Univ. of Notre Dame, Notre Dame, IN, Dec. 1995.
- ¹⁴Hawthorne, W. R., *Aerodynamics of Turbines and Compressors*, Princeton Univ. Press, Princeton, NJ, 1964, p. 225.
- ¹⁵Fabian, M. K., and Jumper, E. J., "Convected and Potential Unsteady Disturbances Interacting with an Unsteady Cascade," AIAA Paper 96-2672, July 1996.
- ¹⁶Fabian, M. K., and Jumper, E. J., "Upstream-Propagating Acoustic Waves Interacting with a Compressible Cascade," AIAA Paper 97-0380, Jan. 1997.
- ¹⁷Capece, V. R., and Fleeter, S., "Experimental Investigation of Multistage Interaction Gust Aerodynamics," *Journal of Turbomachinery*, Vol. 11, Oct. 1989, pp. 409-417.